International Journal of Chemistry; Vol. 9, No. 1; 2017
ISSN 1916-9698 E-ISSN 1916-9701
Published by Canadian Center of Science and Education

The Golden Series and Clusters of Gold-unique Shapes and Bonding

Enos Masheija Rwantale Kiremire[1]

[1]Enos Masheija Rwantale Kiremire, Department of Chemistry and Biochemistry, University of Namibia, Private Bag 13301, Windhoek, Namibia

Correspondence: Enos Masheija Rwantale Kiremire, Department of Chemistry and Biochemistry, University of Namibia, Private Bag 13301, Windhoek, Namibia. E-mail: kiremire15@yahoo.com

Received: November 9, 2016 Accepted: December 12, 2016 Online Published: December 22, 2016

doi:10.5539/ijc.v9n1p38 URL: http://dx.doi.org/10.5539/ijc.v9n1p38

Abstract

Golden clusters have been analyzed and categorized using the series method. They have been found to be intensely capped. The complexity of capping is likely responsible for the unique shapes of clusters. The predicted structures of the golden clusters with one or two nuclear indices have been found to be in agreement with the observations from structural determinations. According to the series, the golden clusters have tendency of occurring in an overlapping area which is normally dominated by naked metal clusters. The series approach method is easy and very reliable in analyzing and characterizing clusters. A brief background to the series method was included to ease readability of the paper.

Keywords: gold-clusters, cluster-code, nuclear-index, cluster-map, 4n-series, Skeletal-numbers, conservation, principle

1. Introduction

The polyhedral skeletal electron pair theory (PSEPT) or simply known as Wade-Mingos rules has been extremely useful in analyzing and categorizing clusters for a long time (Wade, 1971; Mingos, 1972; Welch, 2013). Relatively recently, the 4n series method was developed and has further been refined for rapid application to analyze and characterize clusters with great success (Kiremire, 2016a, 2016b). Golden clusters portray a wide range of fascinating shapes and have attracted increased intensity in research (Cotton and Wilkinson, 1980; Mingos, 1984, 1987; Greenwood and Earnshaw, 1998; Pauling, 1977; Pivoriũnas, 2005; Gimeno, 2008; Konishi, 2014). In addition, gold nanoparticles have shown enormous potential for applications in medicine, catalysis and electronics (Tiwari, et al, 2011; Daniel, et al, 2004). It became tempting to try and analyze the golden clusters using the skeletal numbers derived from 4n series method. This paper presents an analysis and categorization of selected number of golden clusters using the newly introduced skeletal numbers and the conservation of cluster skeletal linkages principle (Kiremire, 2016b).

2. Results and Discussion

2.1 Background

In order to analyze and categorize the gold clusters, the data for skeletal numbers has been reproduced (Kiremire, 2016b) as this is new information for many readers. The skeletal numbers are given in Tables 1 and 2. Their derivation from the series is explained in the same reference (Kiremire, 2016b) and it is not necessary to repeat it in this work. The skeletal numbers have been utilized to calculate the cluster linkage value (K) for a skeletal square pyramid geometry. Selected examples are given in Table 3.

Table 1. Skeletal numbers of main group elements

7.5	7	6.5	6	5.5	5	4.5	4	3.5	3
Sc	Ti	V	Cr	Mn	Fe	Co	Ni	Cu	Zn
Y	Zr	Nb	Mo	Tc	Ru	Rh	Pd	Ag	Cd
La	Hf	Ta	W	Re	Os	Ir	Pt	Au	Hg

Table 2. Skeletal values of transition metals

7.5	7	6.5	6	5.5	5	4.5	4	3.5	3
Sc	Ti	V	Cr	Mn	Fe	Co	Ni	Cu	Zn
Y	Zr	Nb	Mo	Tc	Ru	Rh	Pd	Ag	Cd
La	Hf	Ta	W	Re	Os	Ir	Pt	Au	Hg

2.1.1 Conservation of Cluster Skeletal Linkages Principle

The concept of conservation of cluster skeletal linkages principle is simple. This principle was discovered by careful studies of the 4n series generated when a given cluster of skeletal elements is combined with ligands (Kiremire, 2016b).

The principle simply states that a given cluster comprising of naked skeletal elements contains an inherent fixed number of skeletal linkages. When such a cluster combines with ligands, some or all the skeletal linkages are used up (K_L). Then the sum of the used up linkages and those remaining in the cluster (K_C) are equal to the number of the original linkages (K_O) contained by the naked or uncombined (ligand free) cluster. Using this concept, the skeletal linkages of clusters (K_C) can readily be calculated. A selected sample is given in Table 3. The clusters in Table 3 have been numbered. To illustrate the concept of conservation of cluster skeletal linkages principle, take cluster 1, $K_L + K_C = 17+8 = 25 = K_O$; 6→ $K_L + K_C = 8.5+8 = 16.5 = K_O$; 8→ $K_L + K_C = 4.5+8 =12.5 = K_O$;9 → $K_L + K_C = 3.5+8 = 11.5 = K_O$, and 11→ $K_L + K_C = 6.5+8 =14.5 =K_O$. The beauty and simplicity of the Conservation of Cluster Skeletal Linkages Principle is that for each electron donated to a skeletal fragment by a ligand or simply a naked electron from a charge consumes or removes 0.5 linkage value of the skeletal fragment. Therefore, according to the series, 1H ≡1e (1^-) charge ≡$R^\bullet$(alkyl fragment) ≡ $X^\bullet$ = Cl, Br, I; K = -0.5 and 1 :CO ≡$2H^\bullet$ ≡2e (2^-) charge≡ η^2-C_2H_4 ≡ L = PPh_3, K = 2(-0.5) = -1;η^4-C_4H_4 ≡4e , K = 4(-0.5) = -2; (and η^5-C_5H_5 ≡ 5e, K = 5(-0.5) = -2.5. The negative sign is used for ligands to denote the removal of skeletal values from the naked cluster 'basket'. For example, a boron skeletal element (B) is assigned a K = 2.5(see Table 1). Therefore a B_6 naked skeletal cluster possesses a total of K =6x2.5 = 15 skeletal linkages in its basket. If this skeletal fragment combines with 6H ligands and two negative charges (2e) as ligands, they will consume or remove from the naked B_6 cluster ≡ 6(0.5)+2(0.5) = 4 skeletal linkages. What is left over will be = 15-4 = 11. On the other hand, the osmium cluster, $Os_6(CO)_{18}^{2-}$, the Os skeletal element is assigned K=5(see Table 2). Hence the naked osmium skeletal cluster Os_6 has K =6x5 =30 linkages in its basket. When the naked cluster is combined with 18 CO ligands and 2 negative charges, the linkages removed from its basket will be = 18x1+2(0.5) = 19. What will be left in the Os_6 basket = 30-19 = 11. In this regard, viewing the clusters in this way, it is not a surprise that the skeletal shapes of $B_6H_6^{2-}$ and $Os_6(CO)_{18}^{2-}$ are similar, that is, O_h symmetry as sketched in F-2.

Table 3. Application of skeletal linkage numbers to generate a square pyramid geometry

	CLUSTER	Skeletal Elements	Linkage Contribution By Skeletal Elements, K_o	Ligands	Ligand Linkage Consumption, K_l	Net Cluster Linkages, K_c	n	K(n) code
1	$Ru_5(C)(CO)_{15}$	5Ru	5x5 = 25	1C+15CO	1(2)+15(1) =17	25-17 = 8	5	8(5)
2	$Fe_5(C)(CO)_{14}^{2-}$	5Fe	5x5 =25	1C+14CO+2e	1(2)+14(1)+2(0.5) = 17	25-17 =8	5	8(5)
3	$Fe_5(N)(CO)_{14}^{-}$	5Fe	5x5 =25	1N+14CO+1e	1(2.5)+14(1)+1(0.5)= 17	25-17 =8	5	8(5)
4	$Fe_5(C)(CO)_{12}(L)_3$	5Fe	25	1C+12CO+3L	2+12+3 = 17	25-17=8	5	8(5)
5	L = PMe_2Ph							
6	$(Rh)_2(Cp)_2B_3H_7$	2Rh+3B	2(4.5)+3(2.5) =16.5	2Cp+7H	2(2.5)+7(0.5) = 8.5	16.5-8.5 =8	2+3 = 5	8(5)
7	$Ru_2B_3(Cp)_2(H)_9$	2Ru+3B	2(5)+3(2.5) =17.5	2Cp+9H	2(2.5)+9(0.5) = 9.5	17.5-9.5 =8	2+3 =5	8(5)
8	B_5H_9	5B	5(2.5) =12.5	9H	9(0.5) = 4.5	12.5-4.5 =8	5	8(5)
9	$C_2B_3H_7$	2C+3B	2(2)+3(2.5) =11.5	7H	3.5	11.5-3.5 =8	5	8(5)
10	$C_5H_5^+$	5C	5(2) = 10	5H-1e	2.5-0.5 =2	10-2 = 8	5	8(5)
11	$B_4H_8Co(Cp)$	4B+1Co	4(2.5)+1(4.5) = 14.5	8H+Cp	4+2.5 =6.5	14.5-6.5 =8	5	8(5)
12	$B_4H_8[Fe(CO)_3]$	4B+1Fe	4(2.5)+1(5) =15	8H+3CO	4+3 =7	15-7 =8	5	8(5)
13	$S_2Fe_3(CO)_9$	2S+3Fe	2(1)+3(5) = 17	9CO	9	17-9 =8	5	8(5)
14	$Te_2Fe_3(CO)_9$	2Te+3Fe	17	9CO	9	17-9=8	5	8(5)
15	$Se_2Fe_2Mn(CO)_9^{-}$	2Se+2Fe+1 Mn	2(1)+2(5)+1(5. 5)=17.5	9CO+1e	9.5	17.5-9.5=8	5	8(5)
16	$Re_5(C)(CO)_{16}(H)^{2-}$	5Re	5(5.5)=27.5	1C+16CO+1H+2e	2+16+0.5+2(0.5) =19.5	27.5-19.5 = 8	5	8(5)
17	$Fe_2Mo(CO)_{10}(S)(Te)$	2Fe+1Mo+ 1S+1Te	2(5)+1(6)+1(1) +1(1) =18	10CO	10	18-10 =8	5	8(5)

2.1.2 Derivation of Cluster Series for the Code K(N) and Its Geometry

Given the values of n and the corresponding K value, we can derive the corresponding series. Take the above example of K(n) = 8(5). We know from the series that K = 2n-q/2. Hence, 8 = 2(5)-q/2, q/2 = 10-8 = 2 and q =4. Hence the cluster series is given by S = 4n+q = 4n+4. The 4n+4 series is known as the NIDO family. Therefore all the clusters from 1 to 17 belong to the NIDO family. The K(n) = 8(5) means that the 5 skeletal elements are bound by 8 linkages. The ideal shape of such cluster is normally a square pyramid shown in F-1.

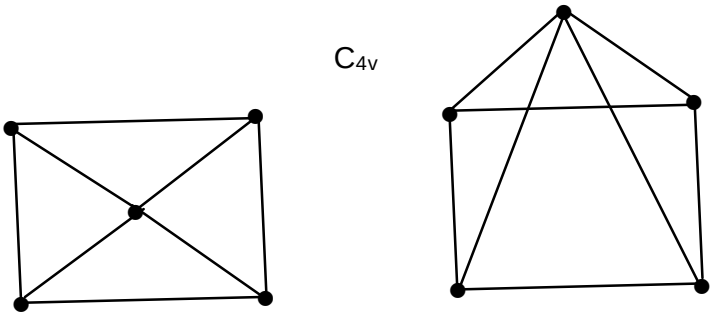

F-1 A sketch of the ideal skeletal shape of K(n) = 8(5)

2.1.3 Valence Electrons of a Cluster

The number of the valence electrons of a cluster is simply derived from the series formula. If the cluster is comprised of main group skeletal elements only, then the series formula is applied as it is. In the case of S = 4n+4, the valence formula becomes V = 4n+4. In the case of K(n) = 8(5), the valence electrons value is, V = 4(5)+4 = 24. In the case of transition elements, V = 14n+4 = 14(5)+4 = 74. If the cluster has mixed skeletal elements, such as cluster number 6 in Table 3, then an adjustment is made to account for this. Using cluster number 6 as an illustration, there 2 transition metal atoms and 3 main group skeletal elements. Therefore, in this case, we use V= 4n+4 = 4(5)+4 = 24. But then since 4n+4 +10n = 14n+4, we have to add 10n = 10(2) = 20 to make allowance for the presence of 2 metal skeletal atoms. Hence, the adjusted number of valence electrons will be given by V = 24+20 = 44. This value can be compared with that calculated from the cluster formula, $Rh_2(Cp)_2B_3H_7$; V = 9x2+5x2+3x3+7 = 44.

Let us consider the transformation of the cluster code from K(n) = 8(5) to 11(6) by adding ΔK(n) = 3(1). The code K(n) = 11(6), gives us K =2(6)-q/2 = 11, q/2 = 1 and q =2.This produces S = 4n+2. The series S = 4n+2 comprises of CLOSO family members. The clusters with a code K(n) = 11(6), normally adopt an ideal octahedral skeletal shape as sketched in F-2. If all the skeletal atoms are transition elements, then the number of valence electrons will be given by V = 14n+2 = 14(6)+2 = 86. A sample of selected clusters with the code K(n) = 11(6) are shown in Scheme 1.

Octahedral, O_h

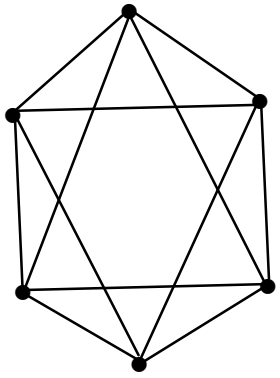

F-2 A sketch of the ideal skeletal shape of K(n) = 11(6)

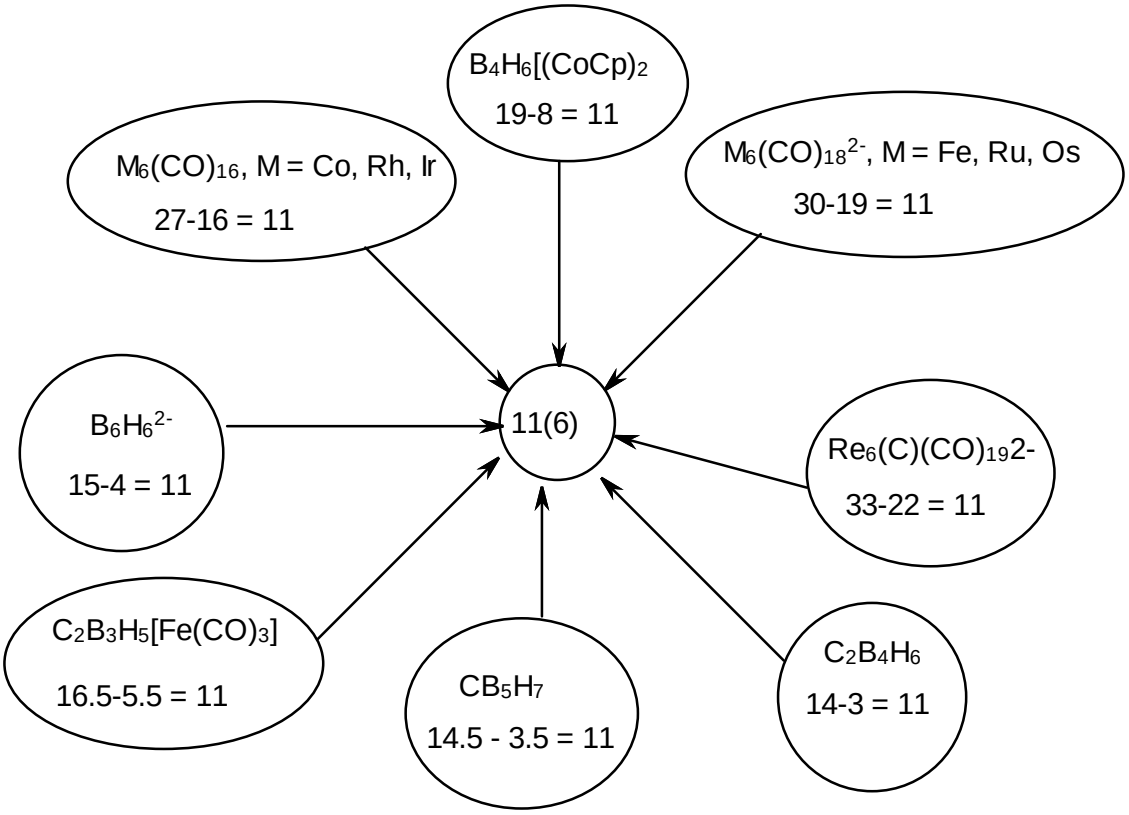

Scheme 1. Some of the cluster systems that generate the ideal O_h symmetry

2.2 Categorization of Golden Clusters

The application of skeletal linkage numbers and the conservation of Cluster Skeletal Linkages Principle, the cluster codes K(n) for golden clusters were determined and hence their respective series. A good number of worked out examples of categorized golden clusters are given in G-0 to G-8 and the rest of the examples are given in a summary form. As can be seen from examples G-1 to G-17, all these golden clusters are intensely capped. The major capping series included C^nC[M-0],n =8-20; C^nC[M-1],n =3-20; C^nC[M-2],n =2-11; C^nC[M-0],n =8-20 and C^nC[M-3],n =3-10. Apart from the 17 golden clusters that have been categorized for illustration, more others were added giving a total of more than 50 clusters and are given in Table 4. It has also been found that those golden clusters centered on one nuclear skeletal element [M-1] are normally referred to as CENTERED TORROIDAL, while those centered on two nuclear skeletal elements, [M-2] are usually referred to as CENTERED SPHERICAL(see Table 8). The capping phenomenon was extensively discussed in previous work (Kiremire, 2016c). In this paper, only brief highlights will be covered by examples. We know that the complex, $Os_6(CO)_{18}^{2-}$ has an octahedral geometry, K = 6(5)-18-1 =11, S = 4n+2(CLOSO family), cluster code =K(n) =11(6)→[M-6] nuclear symbol. A mono-capped cluster of an octahedral osmium complex is $Os_7(CO)_{21}$, K =7(5)-21 =14, S =4n+0, K(n) =14(7), C^1C[M-6]; $Os_8(CO)_{22}^{2-}$,K = 8(5)-22-1 =40-23 = 17, K(n) = 17(8), S =4n-2, C^2C[M-6]→bi-capped octahedral; $Os_9(H)(CO)_{24}^{-}$, K = 9(5)-0.5-24-0.5 = 45-25 =20, K(n) = 20(9), S =4n-4, C^3C[M-6]→tri-capped octahedron, $Os_{10}(CO)_{26}^{2-}$,K =10(5)-26-1 = 50-27 =23, K(n) = 23(10), S =4n-6, C^4C[M-6] tetra-capped octahedron. These examples demonstrate that all these capping clusters have closo nuclei of 6 octahedral skeletal atoms. What is interesting about the golden clusters, is that they do portray clusters whose capping is centered around one skeletal atom (1), [M-1], two skeletal atoms(2), [M-2]or three skeletal atoms(3), [M-3] at the nucleus and in some cases there is no atom in the closo nucleus, [M-0]. This is radically different from the clusters such those of osmium mentioned above whose nuclei are composed of 6 octahedral atoms. There are even giant clusters whose capping is centered around [M-6]. These include $Ni_{38}Pt_6(CO)_{48}(H)^{5-}$(Rossi, et al, 2012); K =38(4)+6(4)-48-0.5-2.5 = 176-51=125,K(n) = 125(44), S =4n-74, $C^{38}C$[M-6], V = 14n-74 = 14(44)-74 = 542 and $Pt_{38}(CO)_{44}^{2-}$,K = 38(4)-44-1 = 152-45 = 107, K(n) = 107(38), S = 4n-62, $C^{32}C$[M-6],V= 14n-62 = 14(38)-62 = 470;$Rh_{23}(CO)_{38}(N)_4^{-}$ (Belyakova, 2003); K =23(4.5)-38-10-0.5 = 103.5-48.5 =55, K(n) =55(23), S =4n-18, $C^{10}C$[M-13].These giant clusters have large "nuclear index". On the other hand, the golden clusters have a tendency of having very small "nuclear indices" regardless as to whether the cluster is of low, medium or high nuclearity. Let us consider the golden cluster (Gimeno,

2008) $Pt(AuL)_8^{2+}$, L =PPh_3. Its K value = 25 has been calculated as shown in G-0 example below. How the 25 linkages are distributed as guided by series is also explained.G-0 $Pt(AuL)_8^{2+}$, L = PPh_3

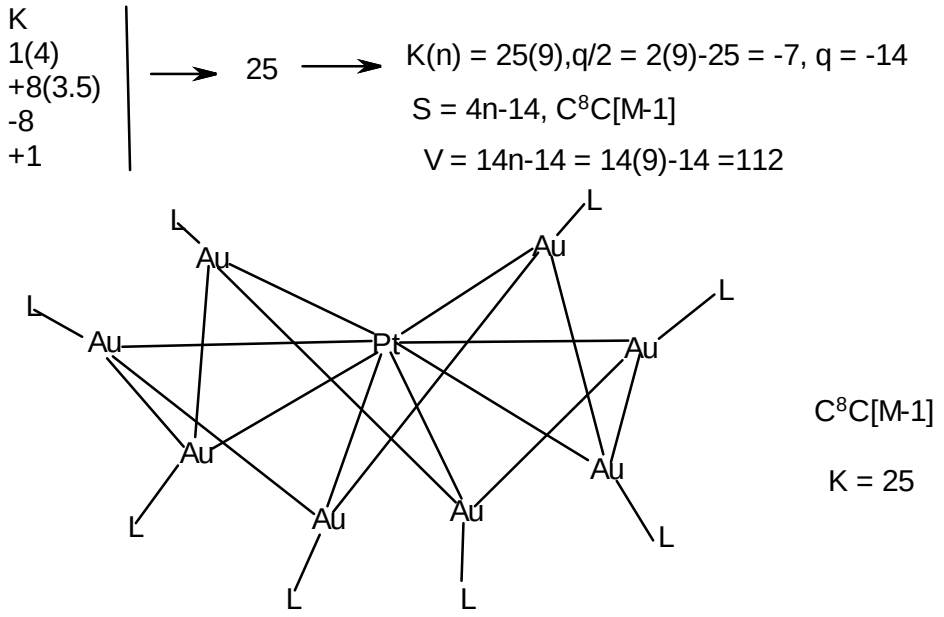

F-3 A skeletal sketch of $Pt(AuL)_8^{2+}$

The series method indicates that one skeletal element will be a CLOSO NUCLEUS and the other 8 skeletal elements will be capped around it. Since the capping linkage of a single skeletal element is derived from the series formula S = 4n-2 and K = 2n+1 = 2(1)+1 =3, this agrees with the 3 connections attached to each of the 8 capping elements. The total linkages associated with 8 skeletal atoms = 3x8 = 24. The [M-1] CLOSO symbol means that the skeletal nucleus atom is a family member of the CLOSO series S = 4n+2, n = 1 and K =2n-1 = 2(1)-1 = 1. This result is quite important because the closo nucleus contains within itself 1 skeletal linkage value K = 1. Thus, $C^8C[M-1]$ is loaded with K = 8x3+1 = 25. In this way, the series method could be regarded as a "miniature microscope" that is utilized to view molecular fragments and clusters however some chemical sense must accompany it for the interpretation of what is observed. This result of K= 25 is in total agreement with the literature report (Gimeno, 2008). A graphical skeletal representation is given in F-3. Suppose the cluster is reacted with a carbonyl ligand to form $Pt(CO)(AuL)_8^{2+}$ complex ,then transformation of thegolden the golden cluster $Pt(AuL)_8^{2+}$ will take place.

$$Pt(AuL)_8^{2+} \xrightarrow{CO} Pt(CO)(AuL)_8^{2+}$$

We know that $Pt(AuL)_8^{2+}$, has K =25. Since a CO ligand is a 2 electron donor, it will remove a value of one (K =1) from the linkage basket of $Pt(AuL)_8^{2+}$. This means that the new K value will have one K value lower, that is, K =25-1 = 24 for $Pt(CO)(AuL)_8^{2+}$ cluster. We can confirm this by the series method of using skeletal linkages, K = 1(4)+8(3.5)-1-8+1= 24, K(n) = 24(9), q/2 =2(9)-24 =-6, q =-12, S = 4n-12, $C^7C[M-2]$, V= 14n-12 =14(9)-12 = 114. The symbol, $C^7C[M-2]$,means that there will be 2 skeletal nuclear atoms surrounded by 7 capping skeletal elements. What has happened is that by removing 1 skeletal linkage, one of the capping skeletal element is forced to uncap and go to the nucleus. This requires skeletal structure re-arrangement. This prediction is observed in the skeletal structure of $Pt(CO)(AuL)_8^{2+}$ reported in literature(Gimeno,2008;Pivoriũnas,2005) and the golden skeletal structure is sketched in F-0(Gimeno, 2008; Pivoriũnas, 2005).

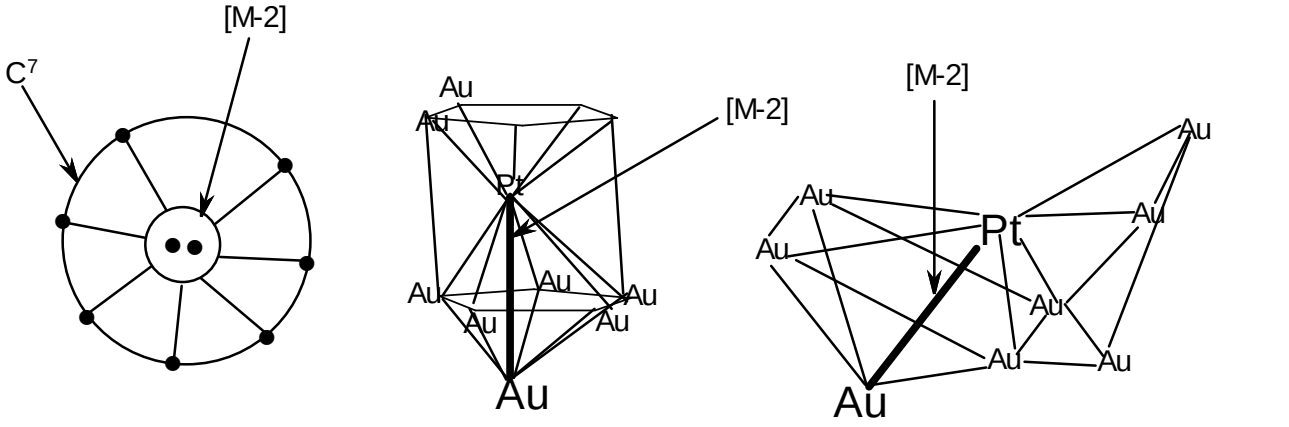

Series prediction Pivoriunas model prediction Observed sketch of $Pt(CO)(AuL)_8^{2+}$

[Pivoriunas,2005] [Gimeno, 2008]

F-0. Graphical sketches of $Pt(CO)(AuL)_8^{2+}$

According to the series, the symbol [M-2] means that the 2 nuclear atoms belong to the CLOSO family, S = 4n+2 and K =2n-1 =2(2)-1 =3. That is, the two nuclear atoms are supposed to be linked by a triple bond, M≡M. It will be interesting to determine which 2 skeletal atoms of the golden cluster are triply bonded. Arising from the complexity of capping and unique geometrical architecture of golden clusters, a desire to construct K(n) cluster map was prompted. The map will facilitate comparing and contrasting the golden clusters with clusters of other transition metals. This resulted in the production of Table 5.

G-1 $Pd(AuL)_8^{2+}$

1(4)
+8(3.5-1)
+2(0.5) $\longrightarrow$ k = 25 , n =1+8 = 9

k = 2n-q/2, q/2 = 2n-k =2(9)-25 = -7, q = -14, S = 4n-14, Cp = $C^1+C^7 = C^8C[M-1]$

G-2 $Pt(AuL)_8^{2+}$ Cp = $C^8C[M-1]$

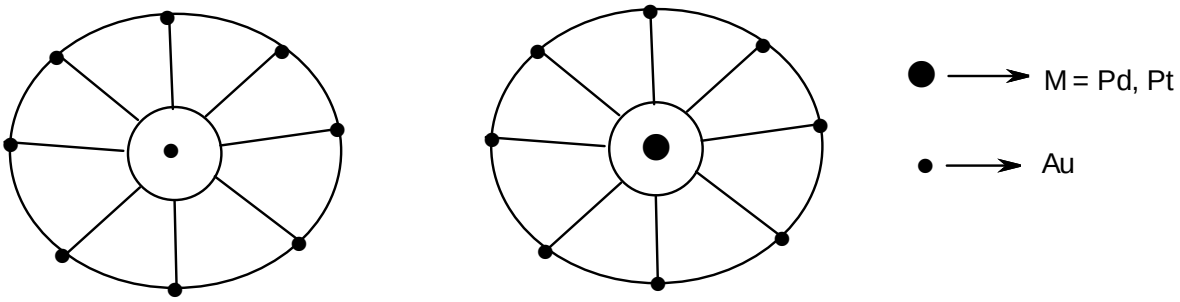

Predicted Observed

F-4 Skeletal sketch of $M(AuL)_8^{2+}$

G-3 $Pd(CO)(AuL)_8^{2+}$

1(4)
+8(3.5-1)
-1
+2(0.5)

→ k = 24 , n =1+8 = 9

k = 2n-q/2, q/2 = 2n-k =2(9)-24 = -6, q = -12, S = 4n-12, Cp = $C^1+C^6 = C^7C[M-2]$

G-4 $Pt(CO)(AuL)_8^{2+}$ Cp = $C^7C[M-2]$

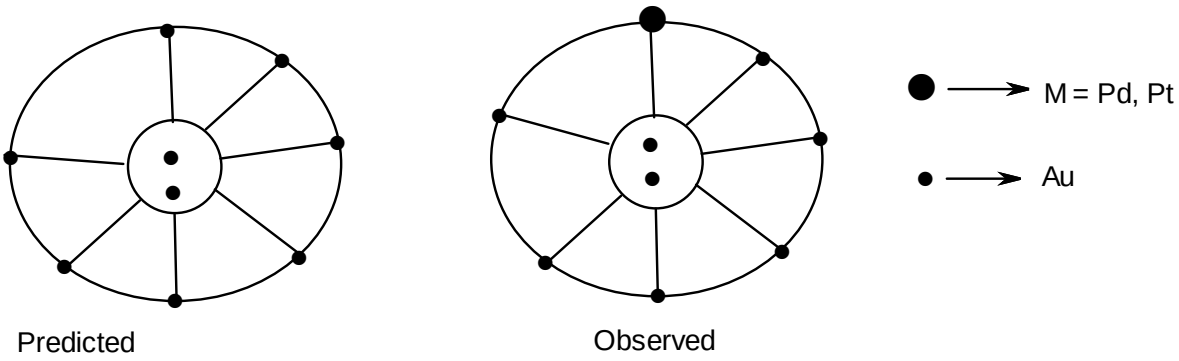

F-5 Skeletal sketch of $M(AuL)_8^{2+}$

G-5 $Au_{10}L_6Cl_3^+$

10(3.5)
-6
-1.5
+1(0.5)

→ k = 28 , n = 10

k = 2n-q/2, q/2 = 2n-k =2(10)-28 = -8, q = -16, S = 4n-16, Cp = $C^1+C^8 = C^9C[M-1]$

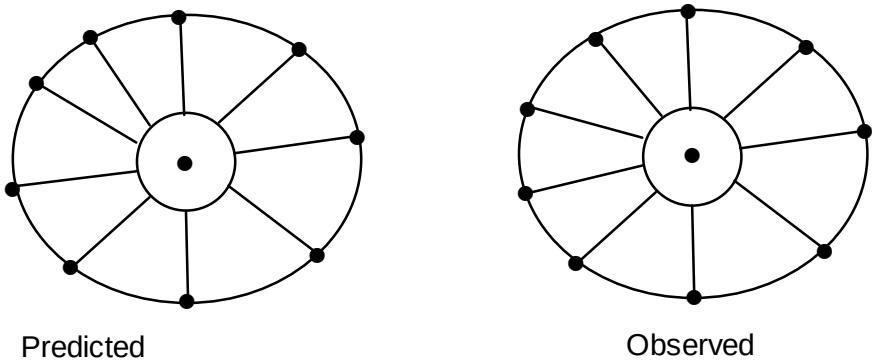

F-6 Skeletal sketch of $Au_{10}L_6Cl_3^+$

G-6 $Au_{10}L_8Cl^+$

10(3.5)
-8
-0.5
+1(0.5)

→ k = 27 , n = 10

k = 2n-q/2, q/2 = 2n-k =2(10)-27 = -7, q = -14, S = 4n-14, Cp = $C^1+C^7 = C^8C[M-2]$

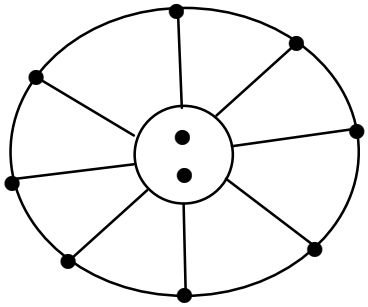

Predicted

F-7 Skeletal sketch of $Au_{10}L_8Cl^+$

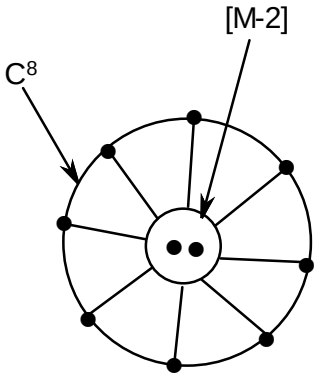

F-7 Observed graph of $Au_{10}L_8Cl^+$

[Konishi, 2014]

Series method

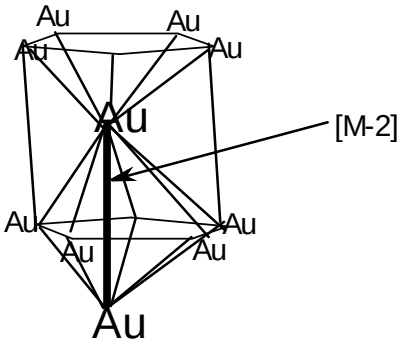

F-7 Skeletal sketch of actual shape of cluster $Au_{10}L_8Cl^+$

[Konishi, 2014]

Pivoriunas model, 2005

G-7 $Au_8L_6^{2+}$

8(3.5)
-6
+1

⟶ k = 23 , n = 8

k = 2n-q/2, q/2 = 2n-k =2(8)-23 = -7, q = -14, S = 4n-14, Cp = $C^1+C^7 = C^8C[M-0]$

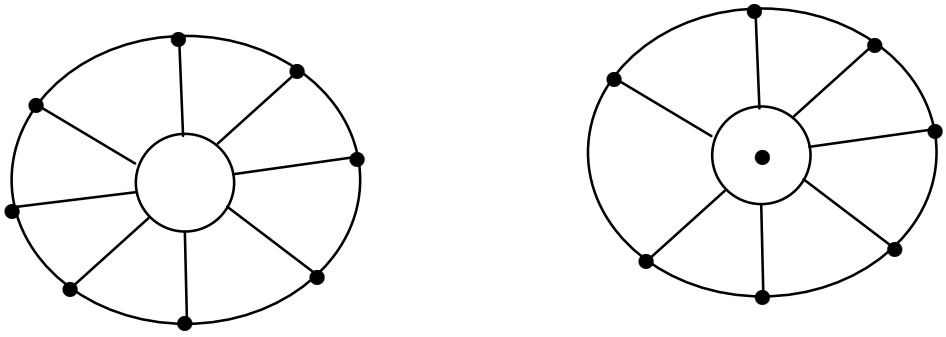

Predicted Observed

F-8 Skeletal sketch of $Au_8L_6^{2+}$

G-8 $Au_8L_8Cl_2^{2+}$ L_2 = dpppe

8(3.5)
-8
-1
+1

⟶ k = 20 , n = 8 k(n) = 20(8)

k = 2n-q/2, q/2 = 2n-k =2(8)-20 = -4, q = -8, S = 4n-8, Cp = $C^1+C^4 = C^5C[M-3]$

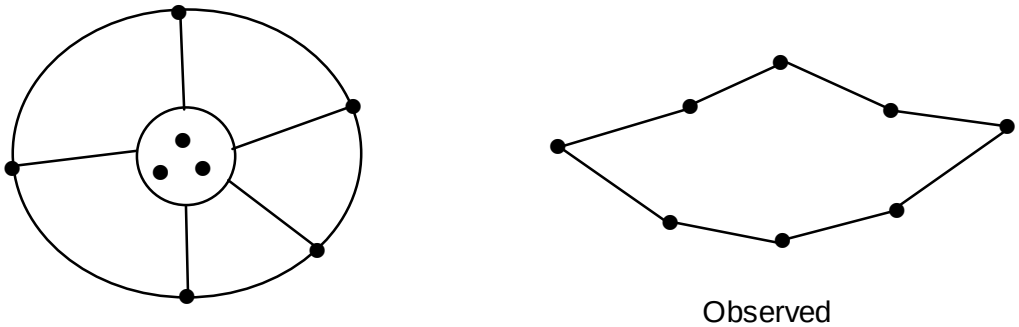

Predicted Observed

F-9 Skeletal sketch of $Au_8L_6Cl_2^{2+}$

G-9 $Au_4(I)_2L_4$, L = PPh_3

k

4(3.5) = 9
-1
-4

k(n) = 9(4), S = 4n-2, Cp = $C^2C[M-2]$

$C^2C[M-2]$

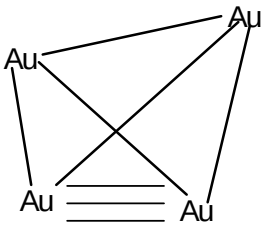

k = 9

F-10

G-10 $Au_6L_6^{2+}$

k = 6(3.5)-6+1 = 16, k(n) = 16(6), S = 4n-8, Cp = $C^5C[M-1]$

V = 14n-8 = 14(6)-8 = 76

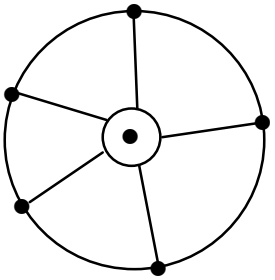

$C^5C[M-1]$

F-11 Rough sketch of predicted structure of G-10

G-11 $Au_7L_7^+$ V = 7x11+7x2-1 = 90

k = 7(3.5)-7+0.5 = 18, k(n) = 18(7), S = 4n-8, $C^5C[M-2]$ V = 14n-8 = 14(7)-8 = 90

Expected Observed [M-2] = 4n+2, k =2n-1 = 2(2)-1 = 3

k = 18

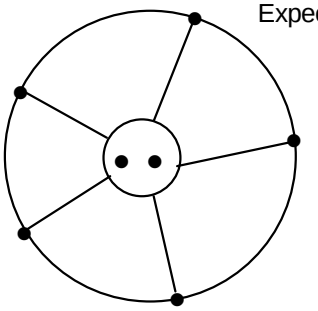

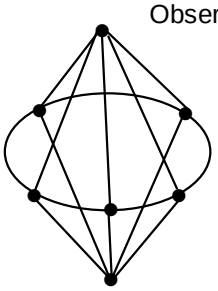

$C^5C[M-2]$

F-12 Sketch of G-11

G-12 $Au_8L_7^{2+}$

L = PPh_3

k = 8(3.5)-7+1 = 22, k(n) = 22(8), S = 4n-12, $C^7C[M-1]$

V = 14n-12 = 14(8)-12 = 100

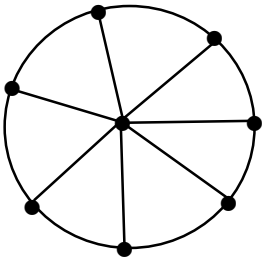

$C^7C[M-1]$

F-13 Graphical skeletal sketch representing G-12

G-13 $Au_9L_8^{3+}$

k(n) = 25(9), S = 4n-14, $C^8C[M-1]$

V = 14n-14 = 14(9)-14 = 112

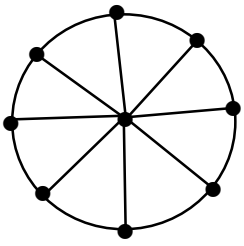

$C^8C[M-1]$

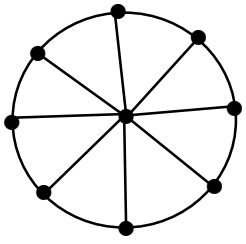

Predicted Observed

F-14 Sketch of graphical skeletal representation of G-13

G-14 $Au_{10}L_6\ Cl_3^+$

k(n) = 28(10), S = 4n-16, $C^9C[M\text{-}1]$

V = 14n-16 = 14(10)-16 = 124

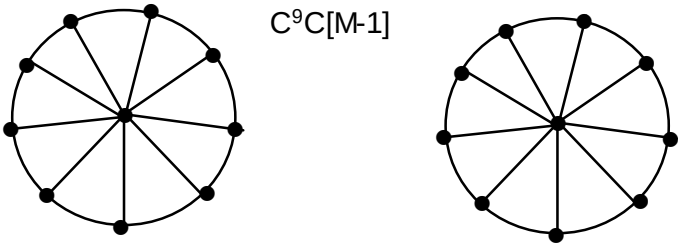

Predicted Observed

F-15 Sketch of graphical skeletal representation of G-14

G-15 $Au_8L_8^{2+}$

k(n) = 21(8), S = 4n-10, $C^6C[M\text{-}2]$

V = 14n-10 = 14(8)-10 = 102

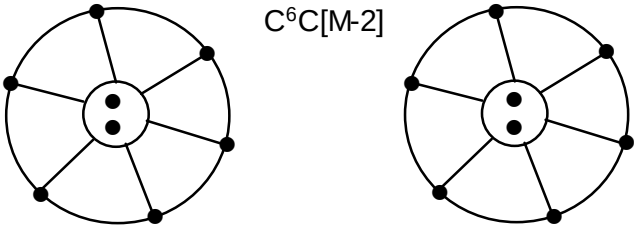

Predicted Observed

F-16 Sketch of graphical skeletal representation of G-15

G-16 $Au_{11}L_7I_3$

k(n) = 30(11), S = 4n-16, $C^9C[M\text{-}2]$

V = 14n-16 = 14(11)-16 = 138

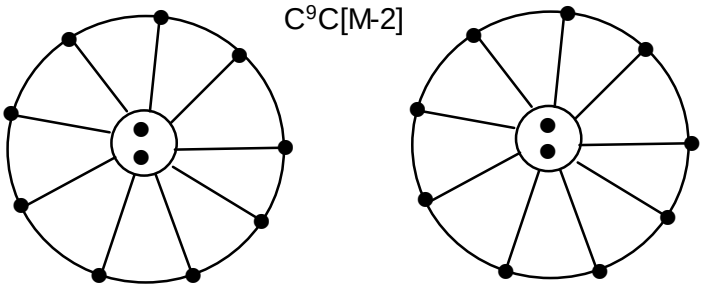

F-17 Sketch of graphical skeletal representation of G-16

G-17 $Au_{13}L_{10}Cl_2^{3+}$

k(n) = 36(13), S = 4n-20, $C^{11}C[M\text{-}2]$

V = 14n-20 = 14(13)-20 = 162

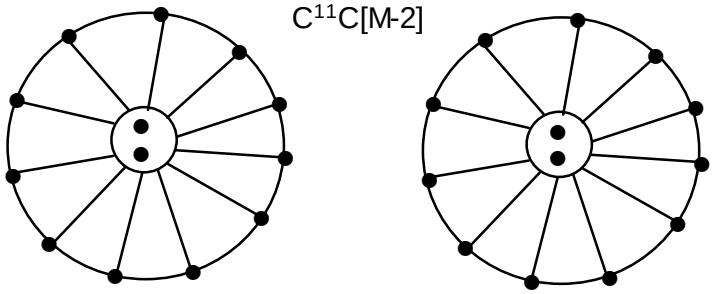

F-18 Sketch of graphical skeletal representation of G-17

Table 4. Selected categorized golden clusters

Cluster	k value	Series	n	V	Category	Code, k(n)
$(AuR)_3(SH)^-$	4	4n+4	3	46	Arachno	4(3)
$Ru_3Cl(CO)_{10}(AuL)$	7	4n+2	4	58	Closo	7(4)
$IrRu_3(CO)_{13}(AuL)$	9	4n+2	5	72	Closo	9(5)
$FeCo_3(CO)_{12}(AuL)$	9	4n+2	5	72	Closo	9(5)
$Au_8L_6^{2+}$	23	4n-14	8	98	C^8C[M-0]	23(8)
$Au_9L_8^{3+}$	26	4n-16	9	110	C^9C[M-0]	26(9)
$Au_{11}L_{10}Cl_2^{3+}$	32	4n-20	11	134	$C^{11}C$[M-0]	32(11)
$Au_{20}L_{10}Cl_4^{2+}$	59	4n-38	20	242	$C^{20}C$[M-0]	59(20)
Au_4L_4	10	4n-4	4	52	C^3C[M-1]	10(4)
$Au_6L_6^{2+}$	16	4n-8	6	76	C^5C[M-1]	16(6)
$Au_6L_4Cl_2$	16	4n-8	6	76	C^5C[M-1]	16(6)
$Au_8L_7^{2+}$	22	4n-12	8	100	C^7C[M-1]	22(8)
$Au_8L_6(I)^+$	22	4n-12	8	100	C^7C[M-1]	22(8)
$Au_9L_8^{3+}$	25	4n-14	9	112	C^8C[M-1]	25(9)
$Au_9L_5R_3$	25	4n-14	9	112	C^8C[M-1]	25(9)
$Pd(AuL)_8^{2+}$	25	4n-14	9	112	C^8C[M-1]	25(9)
$Pt(AuL)_8^{2+}$	25	4n-14	9	112	C^8C[M-1]	25(9)
$Au_{10}L_6Cl_3^+$	28	4n-16	10	124	C^9C[M-1]	28(10)
$Ag_{10}L_8^{2+}$	28	4n-16	10	124	C^9C[M-1]	28(10)
$Au_{11}L_{10}^{5+}$	31	4n-18	11	136	$C^{10}C$[M-1]	31(11)
$Au_{11}L_{10}^{5+}$	31	4n-18	11	136	$C^{10}C$[M-1]	31(11)

Table 4 continued

Cluster	k value	Series	N	V	Category	Code, k(n)
$Au_4L_4I_2$	9	4n-2	4	54	C^2C[M-2]	9(4)
$Au_7L_7^+$	18	4n-8	7	90	C^5C[M-2]	18(7)
$Au_8L_8^{2+}$	21	4n-10	8	102	C^6C[M-2]	21(8)
$Pd(CO)(AuL)_8^{2+}$	24	4n-12	9	114	C^7C[M-2]	24(9)
$Pt(CO)(AuL)_8^{2+}$	24	4n-12	9	114	C^7C[M-2]	24(9)
$Au_9L_8^+$	24	4n-12	9	114	C^7C[M-2]	24(9)
$Au_{10}L_8Cl^+$	27	4n-14	10	126	C^8C[M-2]	27(10)
$Au_{11}L_7Cl_3$	30	4n-16	11	138	C^9C[M-2]	30(11)
$Au_{11}L_8Cl_2^+$	30	4n-16	11	138	C^9C[M-2]	30(11)
$Au_{11}L_{10}^{3+}$	30	4n-16	11	138	C^9C[M-2]	30(11)
$Au_{11}L_8Cl_2^+$	30	4n-16	11	138	C^9C[M-2]	30(11)
$Au_{11}L_{10}^{3+}$	30	4n-16	11	138	C^9C[M-2]	30(11)
$Au_{11}L_7X_3$	30	4n-16	11	138	C^9C[M-2]	30(11)
$Au_{13}L_{10}Cl_2^{3+}$	36	4n-20	13	162	$C^{11}C$[M-2]	36(13)
$Au_{13}L_8Cl_4^+$	36	4n-20	13	162	$C^{11}C$[M-2]	36(13)
$Au_6L_8^{2+}$	14	4n-4	6	80	C^3C[M-3]	14(6)
$Au_8L_8Cl_2^{2+}$	20	4n-8	8	104	C^5C[M-3]	20(8)
$Pd(AuL)_8^{2+}$	23	4n-10	9	116	C^6C[M-3]	23(9)
$Pt(AuL)_8^{2+}$	23	4n-10	9	116	C^6C[M-3]	23(9)
$Au_{13}L_{10}Cl_2^+$	35	4n-18	13	164	$C^{10}C$[M-3]	35(13)
$Au_{11}L_{12}^{3+}$	28	4n-12	11	142	C^7C[M-4]	28(11)
$Pd(AuL)_8(AuCl)_4$	34	4n-16	13	166	C^9C[M-4]	34(13)
$Au_{38}(SR)_{24}$	109	4n-66	38	466	$C^{34}C$[M-4]	109(38)

Table 4 continued

Cluster	k value	Series	n	V	Category	Code
$Au_6L_8^{2+}$	12	4n+0	6	84	C^1C[M-5]	12(6)
$HIrRu_3(CO)_{12}(AuL)_2$	12	4n+0	6	84	C^1C[M-5]	12(6)
$IrRu_3(CO)_{12}(AuL)_3$	15	4n-2	7	96	C^2C[M-5]	15(7)
$Au_{25}(SR)_{18}^-$	69	4n-38	25	312	$C^{20}C$[M-5]	69(25)
$Ru_6(C)(CO)_{16}(AuL)_2$	17	4n-2	8	110	C^2C[M-6]	17(8)
$Os_{10}(C)(CO)_{24}(AuL)^-$	26	4n-8	11	146	C^5C[M-6]	26(11)
$Au_{20}L_{10}Cl_4^{3+}$	49	4n-18	20	262	$C^{10}C$[M-10]	49(20)
$Au_{20}L_9Cl_4^{2+}$	49	4n-18	20	262	$C^{10}C$[M-10]	49(20)
$Au_{22}L_{12}$	55	4n-22	22	286	$C^{12}C$[M-10]	55(22)

Table 5. The K(n) Map of Cluster Series

4n-44	**68(23)**	**70(24)**	**72(25)**	74(26)	76(27)	78(28)	80(29)	82(30)	84(31)	86(32)	C^{23}
4n-42	**65(22)**	**67(23)**	**69(24)**	71(25)	73(26)	75(27)	77(28)	79(29)	81(30)	83(31)	C^{22}
4n-40	**62(21)**	**64(22)**	**66(23)**	68(24)	70(25)	72(26)	74(27)	76(28)	78(29)	80(30)	C^{21}
4n-38	**59(20)**	**61(21)**	**63(22)**	65(23)	67(24)	69(25)	71(26)	73(27)	75(28)	77(29)	C^{20}
4n-36	**56(19)**	**58(20)**	**60(21)**	62(22)	64(23)	66(24)	68(25)	70(26)	72(27)	74(28)	C^{19}
4n-34	**53(18)**	**55(19)**	**57(20)**	59(21)	61(22)	63(23)	65(24)	67(25)	69(26)	71(27)	C^{18}
4n-32	**50(17)**	**52(18)**	**54(19)**	56(20)	58(21)	60(22)	62(23)	64(24)	66(25)	68(26)	C^{17}
4n-30	**47(16)**	**49(17)**	**51(18)**	53(19)	55(20)	57(21)	59(22)	61(23)	63(24)	65(25)	C^{16}
4n-28	**44(15)**	**46(16)**	**48(17)**	50(18)	52(19)	54(20)	56(21)	58(22)	60(23)	62(24)	C^{15}
4n-26	**41(14)**	**43(15)**	**45(16)**	47(17)	49(18)	51(19)	53(20)	55(21)	57(22)	59(23)	C^{14}
4n-24	**38(13)**	**40(14)**	**42(15)**	44(16)	46(17)	48(18)	50(19)	52(20)	54(21)	56(22)	C^{13}
4n-22	**35(12)**	**37(13)**	**39(14)**	41(15)	43(16)	45(17)	47(18)	49(19)	51(20)	53(21)	C^{12}
4n-20	**32(11)**	**34(12)**	**36(13)**	38(14)	40(15)	42(16)	44(17)	46(18)	48(19)	50(20)	C^{11}
4n-18	**29(10)**	**31(11)**	**33(12)**	35(13)	37(14)	39(15)	41(16)	43(17)	45(18)	47(19)	C^{10}
4n-16	**26(9)**	**28(10)**	**30(11)**	32(12)	34(13)	36(14)	38(15)	40(16)	42(17)	44(18)	C^{9}
4n-14	**23(8)**	**25(9)**	**27(10)**	29(11)	31(12)	33(13)	35(14)	37(15)	39(16)	41(17)	C^{8}
4n-12	**20(7)**	**22(8)**	**24(9)**	26(10)	28(11)	30(12)	32(13)	34(14)	36(15)	38(16)	C^{7}
4n-10	**17(6)**	**19(7)**	**21(8)**	23(9)	25(10)	27(11)	29(12)	31(13)	33(14)	35(15)	C^{6}
4n-8	**14(5)**	**16(6)**	**18(7)**	20(8)	22(9)	24(10)	26(11)	28(12)	30(13)	32(14)	C^{5}
4n-6	**11(4)**	**13(5)**	**15(6)**	17(7)	19(8)	21(9)	23(10)	25(11)	27(12)	29(13)	C^{4}
4n-4	**8(3)**	**10(4)**	**12(5)**	14(6)	16(7)	18(8)	20(9)	22(10)	24(11)	26(12)	C^{3}
4n-2	**5(2)**	**7(3)**	**9(4)**	11(5)	13(6)	15(7)	17(8)	19(9)	21(10)	23(11)	C^{2}
4n+0	**2(1)**	**4(2)**	**6(3)**	8(4)	10(5)	12(6)	14(7)	16(8)	18(9)	20(10)	C^{1}
4n+2	[-1](0)	1(1)	3(2)	5(3)	7(4)	**9(5)**	**11(6)**	13(7)	15(8)	17(9)	closo
[M-x]	**M-0**	**M-1**	**M-2**	**M-3**	**M-4**	**M-5**	**M-6**	**M-7**	**M-8**	**M-9**	4n+2
4n+4			0(1)	2(2)	4(3)	**6(4)**	**8(5)**	10(6)	12(7)	14(8)	Nido
4n+6	*	*	*		1(2)	**3(3)**	**5(4)**	7(5)	9(6)	11(7)	Arac

2.3 Construction of Table 5

In Scheme 1, the code k(n) =11(6) was used as a unifying point for all clusters with the ideal octahedral symmetry. Taking this code as an example, k = 11 refers to the skeletal linkages the cluster has and n = 6 refers to the number of skeletal atoms. Numerous cluster complexes with the ideal octahedral could be cited which fulfill the requirement k(n) = 11(6). Thus this code unites all the family members which possess an octahedral shape. However, some cases with k(n) = 11(6) may not have an ideal octahedral shape. Such shapes may be considered to portray some form of "k-isomerism. From the series we know that a capping step involves a change $\Delta n = 1$ and $\Delta k = 2n+1 = 2(1)+1 = 3$, then we can easily construct a column of capping series in terms of the cluster code k(n) for an ideal octahedral system as follows: 11(6)→14(7) →17(8) →20(9) →23(10) →26(11) →29(12), and so on. Starting from 11(6), we can extend the column downwards as follows: 11(6) →8(5) →5(4) →2(3) →-1(2). The k(n) = -1(2) makes little chemical sense and therefore it is not necessary to go beyond this point. In earlier work (Kiremire, 2016c), the capping osmium carbonyl fragment was found to be $Os(CO)_3$, S = 14n-2, k = 2n+1=3, V = 14 and it involves changing the type of series. However the horizontal movement along the row the type of series remain the same and $\Delta n = \pm 1$ and $k = \pm 2$. Taking the k(n) = 11(6) as an illustration, and moving horizontally along the row, from left to right, we get the series 11(6)→13(7) →15(8) →17(9) →19(10) and so on. Starting from 11(6) and moving from right to left we get the CLOSO series 11(6)→9(5) →7(4) →5(3) →3(2) →1(1) →-1(0). In principle, starting from one k(n) code, an infinite array of k(n) values can be constructed. Table 5 is extremely important and may be regarded as a "map" of clusters. Let us consider the following cluster codes taken from Table -5**;** 10(4), 16(6), 22(8), 25(9), 28(10) and 31(11). All these code lie on [M-1] axis while the codes 9(4), 18(7), 21(8), 24(9), 27(10), 30(11) and 36(13) lie on [M-2] axis. Clearly, all these golden cluster codes are located on the far left of the cluster code map(Table 5). The K(n) parameter in table 5 means that (k)stands for cluster linkages while the(n) in parenthesis stands for the number of the skeletal elements corresponding to that k value. The middle region of the cluster map and the extreme right of the map is the area occupied mainly by the transition metal clusters. The clusters such as boranes, hydrocarbons, and main group elements clusters lie bellow the CLOSO AXIS and are on the right portion of the cluster code map. This is summarized in Table-6. Thus, Table 6 is a derivative of Table 5. The significance of the table is that it shows that the clusters of the 'lower' series such as boranes and hydrocarbons (nido, arachno, klapo) are rare or non-existent on the extreme left side of the table. Only one possible member, K(n) = 2(2) appears at [M-3] column(see Table 5). The closo nuclear baseline [M-x] is shown in red while its corresponding K(n) values along S = 4n+2 are shown in blue color above it. Also shown in blue below the [M-x] axis are the K(n) values corresponding to 4n+4 and 4n+6 series. The number of lower series clusters increases as the nuclear [M-x] index (x) increases from 4 to values of x>4. In addition, a capping code, $C^nC[M\text{-}x]$ may be expressed as point on the vertical axis as illustrated in Table 7. The degree of cluster capping increases as you move from right to the left in Table 5. As can be seen from Table 2, the 'periodic law' of the skeletal numbers decreases from left to right starting with

k value of 7.5 to k value of 3. Gold belongs to a period with a k value of 3.5. It appears that the lower the k value of the skeletal element, the greater the tendency of the element form capping clusters with low nuclear indices. This is probably the reason why Au forms capping series with [M-1] and [M-2] nuclear indices. If in the cluster code K(n), if we keep n constant and move along a diagonal from the right to the left the K value increases stepwise by one. This means that capping becomes more and more intense as we move along a diagonal from left to right in Table 5. Take the example K(n) = 9(6) in Table 5. This code represents clusters such as C_6H_6, which has isomers such as benzene and prismane or $Co_6(P)(CO)_{16}^{-}$. The diagonal movement left-wise, we get the sequences of cluster codes as follows; 9(6)→10(6) →11(6)[octahedral clusters) →12(6)[mono-capped trigonal bipyramid→13(6) →14(6) →15(6) →16(6). When we reach at K(n) = 16(6), we encounter clusters such as $Au_6L_6^{2+}$, L = PPh_3. At K(n)= 9(6), q/2 = 2(6)-9 = 3, q = 6, S =4n+6 (ARACHNO family)[Trigonal Prism skeletal shape] while at K(n) = 16(6), q/2 = 2(6)-16 = -4, q = -8, S = 4n-8, C^5C[M-1][Penta-capped mono-nuclear cluster]. This is a major transformation in symmetry. That is why the skeletal shape of $Co_6(P)(CO)_{16}^{-}$ (K = 9) is radically different from that of $Au_6(PPh_3)_6^{2+}$(K =16).

2.4 Geometries and Bonding in Golden Clusters

Arising from the complexity of the capping nature of gold clusters, their geometries and nature of bonding are expected to be complex. This will be illustrated by considering a few examples. Consider the cluster $Au_4(I)_2(L)_4$, L =PPh_3 is described as having a tetrahedral geometry(Mingos, 1984). The cluster has a k value of 9. This means it embodies 9 skeletal linkages within 4 skeletal elements, with a code k(n) = 9(4). The cluster belongs to S = 4n-2 series with the capping Cp = C^2C [M-2]. According to the 4n series, this means the cluster has two skeletal elements which are capping on other 2 atoms which are linked by a triple bond as indicated in F-10. On the other hand a transition metal carbonyl cluster such as $Ir_4(CO)_{12}$, k = 6, code k(n) = 6(4), S = 4n+4. This means it belongs to the nido series. This cluster has 4 skeletal elements bound by 6 linkages as shown in F-2. The skeletal shape is expected to have a genuine tetrahedral symmetry. Clearly, there is a fundamental difference between k(n) = 9(4) and k(n) =6(4). The difference can be traced on the k(n) diagonal:6(4)→7(4) →8(4) →9(4). The 6(4) lies in the nido region while 9(4) lies in the bi-capped region close to naked metal cluster region. Another good example is $Au_6L_6^{2+}$(L = PPh_3). This cluster is described as having an octahedral skeletal geometry (Cotton, et al, 1980; Mingos, 1984). But the cluster has a k value of 16, k(n) = 16(6) and belongs to S = 4n-8 series with Cp = C^5C[M-1]. The k =16 can readily be calculated from the cluster formula as follows: k =6(3.5)-6+1 = 16 and the series formula derived as explained in examples G-1 to G-8. As we have seen, an ordinary octahedral shape has k(n) = 11(6) code, and S = 4n+2, closo. Let us trace the changes in series from 11(6) to 16(6). The series are 11(6) →4n+2, 12(6) →4n+0, 13(6) →4n-2, 14(6) →4n-4, 15(6) →4n-6, and 16(6) →4n-8, Cp = C^5C[M-1]. This means the cluster is expected to have one nuclear element with a cluster content k = 1 surrounded by 5 capped skeletal elements with 15 linkages. These changes can be traced diagonally in Table 4A. In short, the gold cluster k(n) = 16(6) of 6 skeletal elements and 16 linkages is expected to have a much more complex structure than, k(n) = 11(6) with 6 skeletal atoms and 11 linkages. Following the procedure adopted in sketching the sketch F-3 adopted from the literature (Gimeno, 2008), we can produce a possible tentative shape of the yellow cluster (Cotton, et al, 1980) $Au_6L_6^{2+}$ as indicated in F-z guided by k values from the series. The skeletal atom around which other 5 elements are capped has been enlarged for emphasis. In three dimensional set up, the shape gives a semblance of an octahedral geometry.

C^5C[M-1] ⟶ K = 5x3+1 = 16

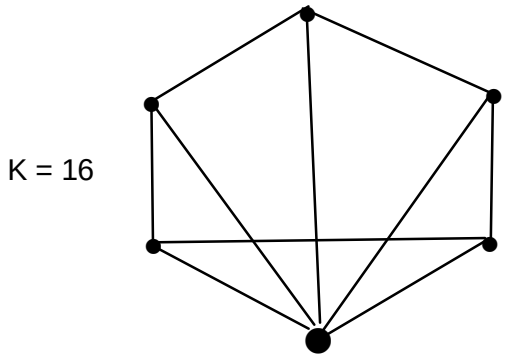

F-z Tentative possible sketch of $Au_6L_6^{2+}$

Consider another good example, $Au_7L_7^{+}$; k(n) = 18(7), S =4n-8, Cp = C^5C[M-2]. If we assume that the 5 skeletal atoms are capped around two others joined by a triple bond, then we can represent this by a proposed possible skeletal sketch shown in F-19.

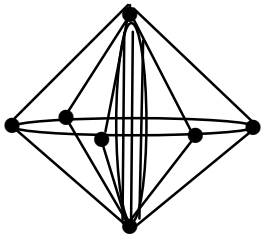

F-19

Surprisingly, this geometrical model was found to be in agreement with that of Pivoriũnas (Pivoriũnas, 2005). The cluster has been described as pentagonal bipyramid (Mingos, 1984). According to the 4n series, it has two atoms linked by a triple bond around which 5 other skeletal elements are joined by 15 linkages. An ordinary pentagonal bipyramid cluster such as $B_7H_7^{2-}$, k(n) = 13(7), has seven skeletal atoms with a content of 13 linkages as opposed to 18 linkages for the 7 golden skeletal atoms.

Let us take one more example $Au_{10}Cl_3L_6^+$. This cluster has a cluster code k(n) = 28(10) with S = 4n-16, V = 14n-16 = 124 and Cp = $C^9C[M-1]$. According to 4n series, this cluster has one skeletal atom at the nucleus around which 9 other skeletal elements are capped with a total of 28 skeletal linkages. Indeed this is what is observed (Mingos, 1984; Konishi, 2014). A rough skeletal sketch of this is shown in F-20. Mingos describes clusters of this nature as follows "The higher nuclearity clusters are characterized by the presence of an additional central gold atom and the presence of this atom makes a fundamental contribution to the bonding because the radial metal-metal bonding to the central metal atom is stronger than the peripheral metal-metal bonding on the surface of the cluster" (Mingos, 1984). This powerful statement underpins the power of series method.

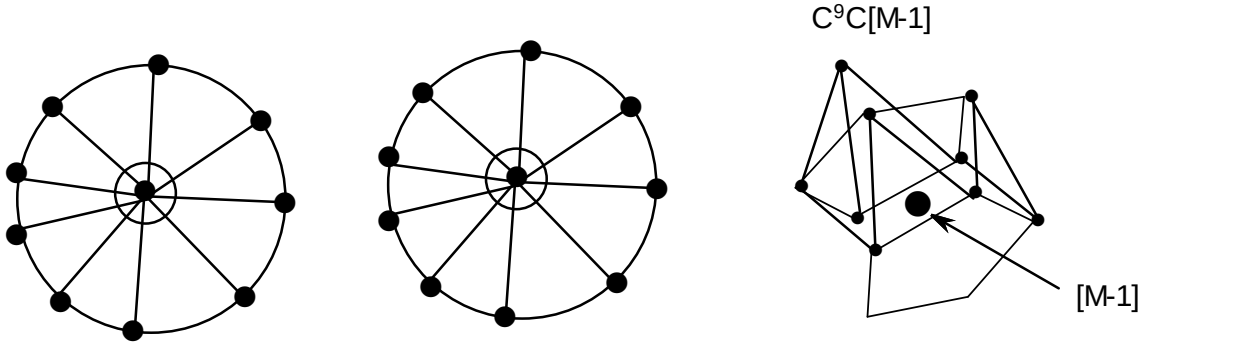

F-20. Graphical sketches of $Au_{10}Cl_3L_6^+$

2.5 Observing the Nuclear Centers of Clusters.

The capping symbol that was introduced in earlier work is $C^nC[M-x]$. The [M-x] is the cluster nucleus. The value of x = 1, 2, 3, 4, 5, 6, 7, 8, 9, 10 and so on represent the number of skeletal elements present in the nucleus. What has been witnessed in the gold clusters are some of the clusters of the type $C^nC[M-1]$ given the name single atom-centered toroidal clusters. For giant clusters, nuclei such as $C^nC[M-x](x>6)$ have been encountered. It will be interesting if the atoms which constitute [M-x] nuclei could easily be identified by x-ray structural analysis as predicted by the series approach.

Table 6. Sketch to show the relative positions of clusters on the K(n) map

	10	
	9	
	8	
NAKED METAL	7	
GOLD CLUSTERS(x = -4→0)	6	GOLD CLUSTERS(x = 0→4)
	5	
	4	
	3	
	2	TRANSITION METAL CARBONYLS(x = 0→ ABOVE)
	1	METALLOBORANES(x = 0 →ABOVE)
[M-x] -5 -4 -3 -2 -1	0	1 2 3 4 5 6 7 8 9 10 11 12
CLOSO, NIDO,ARACHNO, KLAPO		CLOSO BORANES(x = 1→ABOVE)
NON-EXISTENT		NIDO CARBORANES(x = 1→ABOVE)
		ARACHNO METALLOBORANES(x = 1→ABOVE)
		HYPHO METALLACARBORANES(x = 1→ABOVE)
		KLAPO ZINTL IONS(x = 1→ABOVE)
		HYDROCARBONS(x = 1→ABOVE)
		TRANSITION METAL CARBONYLS(x = 1→ABOVE)
		MAIN GROUP ELEMENT CLUSTERS(x = 1→ABOVE)
		NON-CAPPING REGION

Table 7. Geometrical representation of capping cluster on a given [M-x] column

C^{20}	20			
C^{19}	19			
C^{18}	18			
C^{17}	17			
C^{16}	16			
C^{15}	15			
C^{14}	14			
C^{13}	13			
C^{12}	12			
C^{11}	11	(0,11)	(1,10)	(2,11)
C^{10}	10			
C^{9}	9	(0,9)	(1,9)	(2,9)
C^{8}	8	(0,8)	(1,8)	(2,8)
C^{7}	7		(1,7)	(2,7)
C^{6}	6			
C^{5}	5		(1,5)	(2,5)
C^{4}	4			
C^{3}	3		(1,3)	
C^{2}	2			(2,2)
C^{1}	1			
[M-x]	0	1	2	

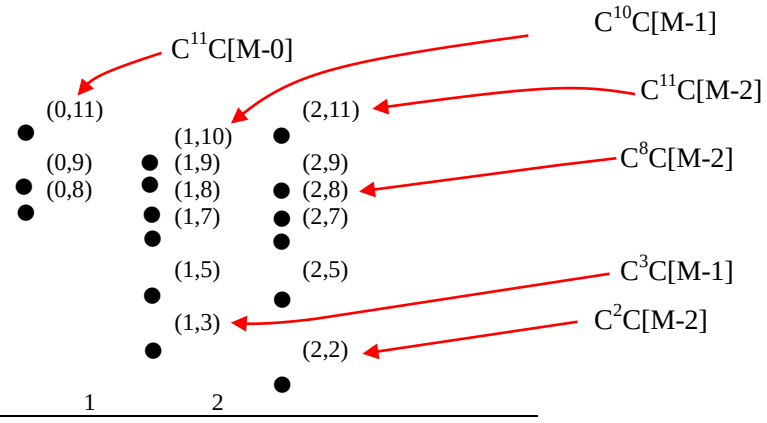

Table 8. Comparing series results of a selected sample of golden clusters with literature information

T-8	COMPARE									
Cluster	k value	Series	n	V series	Category Series	Code, k(n)	Lit.	Lit.	V Lit.	Ref.
$Au_4L_4I_2$	9	4n-4	4	54	C^2C[M-2]	9(4)	tetrahedral		54	1
$Au_6L_6^{2+}$	16	4n-8	6	76	C^5C[M-1]	16(6)	octahedral		76	1,2,3
				90		18(7)	Pentagonal		88	1
$Au_7L_7^{+}$	18	4n-8	7		C^5C[M-2]		bipyramid			
$Au_6L_8^{2+}$	14	4n-4	6	80	C^3C[M-3]	14(6)	Di-edge-bridged T_d		80	1
				100		22(8)	Icosahedron	Centered	100	1
$Au_8L_7^{2+}$	22	4n-12	8		C^7C[M-1]			TOR		
				112		25(9)		Centered		
$Au_9R_3L_5$	25	4n-14	9		C^8C[M-1]			TOR		
				112		25(9)	Centered crown	Centered	112	1,2,3
$Au_9L_8^{3+}$	25	4n-14	9		C^9C[M-1]			TOR		
				102		21(8)	Capped centered	Centered	102	1
$Au_8L_8^{2+}$	21	4n-10	8		C^6C[M-2]		chair	SP		
				114		24(9)	Bi-capped centered		114	1
$Au_9L_8^{+}$	24	4n-12	9		C^7C[M-2]		chair			
				124		28(10)		Centered		1
$Au_{10}L_6Cl_3^{+}$	28	4n-16	10		C^9C[M-1]			TOR		
				138		30(11)	Dodecahedron	Centered	128	1,2,3
$Au_{11}L_7X_3$	30	4n-16	11		C^9C[M-2]			SP		
				162		36(13)	Icosahedron	Centered	152	1
$Au_{13}L_{10}Cl_2^{3+}$	36	4n-20	13		$C^{11}C$[M-2]			SP		

TOR = TORROIDAL, SP = SPHERICAL, 1 = Mingos, 1984; 2 =Pauling,1977; 3 =Cotton, et al, 1980

3. Conclusion

Elemental gold forms clusters which are intensely capped. According to series approach, they tend to occur in a region overlapping with the area where naked metallic clusters are normally found. Although a good range of clusters have nuclei of the type [M-x], x = 1 or 2 (centered toroidal or centered spherical), x can take up values, 3, 4, 5, 6 and so on. But the majority of clusters are congested around x = 0-4 region. The series are quite reliable in analyzing and categorizing a wide range of clusters. A lot more needs to be done to fully understand the unique shapes and bonding in the golden clusters which portray complex capping even for a small number of skeletal atoms. Indeed, gold cluster chemistry is a rich mine of knowledge, yet much more waiting to be mined.

Acknowledgement

The financial assistance by the University of Namibia and NAMSOV, Namibia is greatly appreciated. Mrs Merab Kambamu Kiremire for proof-reading the draft is hereby acknowledged.

Dedication

This work is dedicated to two of the great historical scientists, namely Irving Langmuir and Gilbert Newton Lewis for their brilliant insights and contributions towards the 18 and 8 electron rules more than 90 years ago.

References

Belyakova, O. A., & Slovokhotova, Y. L. (2003). Structures of large transition metal clusters. Russian Chemical Bulletin. Inter. Ed., *52*(11), 1-29. https://doi.org/10.1023/B:RUCB.0000012351.07223.d4

Cotton, F. A., & Wilkinson, G. (1980). *Advanced Inorganic Chemistry, 4th Ed.*, John Wiley and Sons, New York, 1980.

Daniel, M. C., & Astruc, D. (2004). Gold Nanoparticles, Assembly, Supramolecular Chemistry, Quantum-Size-Related Properties, and Applications toward biology, Catalysis and Nanotechnology. *Chem. Rev.*, *104*, 293-346. https://doi.org/10.1021/cr030698+

Gimeno, M. C. (2008). Modern Supramolecular Gold-Metal Interactive and Applications. Edited A. Laguna, 2008. Wiley-VCH, Weinheim.

Greenwood, N. N., & Earnshaw, A. (1998). *Chemistry of the Elements, 2nd Ed*. Butterworth, Oxford.

Kiremire, E. M. R. (2016a). The Application of the 4n Series Method to Categorize Metalloboranes. *Int. J. Chem.*, *8*(3), 62-73. https://doi.org/10.5539/ijc.v8n3p62

Kiremire, E. M. R. (2016b). A Hypothetical Model for the Formation of Transition metal Carbonyl Clusters Based Upon 4n Series Skeletal Numbers. *Int. J. Chem.*, *8*(4), 78-110. https://doi.org/10.5539/ijc.v8n4p78

Kiremire, E. M. R. (2016c). Unusual underground capping Carbonyl Clusters of Palladium. *Int. J. Chem.*, *8*(1), 145-158. https://doi.org/10.5539/ijc.v8n1p145

Konishi, K. (2014). Phosphine-Coordinated Pure-Gold Clusters and Unique Optical Properties /Responses. Structure and Bonding, *161*, 49-86. https://doi.org/10.1007/430_2014_143

Mingos, D. M. P. (1972). A General Theory for Cluster and Ring Compounds of the Main Group and Transition Elements. *Nature (London), Phys. Sci., 236*, 99-102. https://doi.org/10.1038/physci236099a0

Mingos, D. M. P. (1984). Gold Cluster Compounds: Are they materials in miniature? *Gold Bull., 17*(1), 5-12. https://doi.org/10.1007/bf03214670

Mingos, D. M. P. (1987). Complementary spherical electron density model for coordination compounds. *Pure and Appl. Chem., 59*(2), 145-154. https://doi.org/10.1351/pac198759020145

Pauling, L. (1977). Structure of Transition Metal Cluster Compounds: Use of an additional orbital resulting from f, g character of SPD bond orbitals. *Proc. Natl. Acad. Sci., USA, 74*(12), 5235-5238. https://doi.org/10.1073/pnas.74.12.5235

Pivoriunas, G. (2005). Neuer Goldcluster. PhD Thesis

Rossi, F., & Zanello, P. (2011). Electron Reservoir Activity of High-Nuclearity Transition Metal Carbonyl Clusters. *Portugalia, Electrochimica Acta, 29*(1), 309-327. https://doi.org/10.4152/pea.201105309

Tiwari, P. M., Vig, K., Dennis, A., & Sing, S. R. (2011). Functionalized Gold Nanoparticles and Their Biomedical Applications. Nanomaterials, *1*, 31-63. https://doi.org/10.3390/nano1010031

Wade, K. (1971). The structural significance of the number of skeletal bonding electron-pairs in carboranes, the higher boranes and borane ions and various transition metal carbonyl cluster compounds. *Chem. Commun.,* 792-793. https://doi.org/10.1039/c29710000792

Welch, A. J. (2013). The significance of Wade's rules. *Chem. Commun., 49*, 3615-3616. https://doi.org/10.1039/c3cc00069a